Research Square

Preprints are preliminary reports that have not undergone peer review.
They should not be considered conclusive, used to inform clinical practice,
or referenced by the media as validated information.

Structural Reliability of a Cessna 172 Main Wing Spar under Dynamic Excitation Using Monte Carlo Simulation

Marcelo Araujo da Silva

marcelo.araujo@ufabc.edu.br

Universidade Federal do ABC

Ivan Pedroso

Universidade Federal do ABC

Jean Vasco

Universidade Federal do ABC

Research Article

Keywords: Structural reliability, Monte Carlo simulation, Wing spar, Independent random variables

Posted Date: September 4th, 2026

DOI: https://doi.org/10.21203/rs.3.rs-10744608/v1

License: This work is licensed under a Creative Commons Attribution 4.0 International License.
Read Full License

Additional Declarations: No competing interests reported.

Structural Reliability of a Cessna 172 Main Wing Spar under Dynamic Excitation Using Monte Carlo Simulation

Marcelo Araujo da Silva[1*], Ivan Pedroso[1] and Jean Vasco[1]

[1*]Center for Engineering, Modeling and Applied Social Sciences, Federal University of ABC, Av. dos Estados, Santo André, 09280-560, São Paulo, Brazil.

*Corresponding author(s). E-mail(s): marcelo.araujo@ufabc.edu.br;

Abstract

This paper presents a probabilistic assessment of a Cessna 172 main wing spar subjected to uncertain aerodynamic loading and harmonic excitation. The spar is modeled as a cantilever Euler-Bernoulli beam with an I-shaped cross-section made of 2024-T3 aluminum alloy. The uncertainty model considers independent random variables for geometry, material properties, aerodynamic load, and excitation frequency, with Gaussian distributions for structural parameters and a uniform distribution for frequency within prescribed bands. Internal forces are obtained from an elliptical lift distribution, and stresses are evaluated using the Von Mises criterion with dynamic amplification based on modal frequency response. Results show that reliability is strongly affected by resonance, with the second and third vibration modes producing the most critical excitation bands. A broad-band analysis from 0 to 200 Hz resulted in a failure probability of 0.852% and a reliability index of 3.38, highlighting the importance of resonance in aerospace structural reliability assessment under dynamic uncertainties.

Keywords: Structural reliability, Monte Carlo simulation, Wing spar, Independent random variables

1 Introduction

Aircraft wing spars are primary load-carrying members that transfer aerodynamic lift from the wing to the fuselage [1]. Their structural performance is affected by

uncertainties in geometry, material properties, loading, and dynamic excitation, making reliability analysis an appropriate tool to quantify the margin between structural capacity and demand [2].

This work presents a condensed version of the original research report, focusing on the main spar of a Cessna 172 Skyhawk. The analysis combines a simplified structural model, an elliptical lift distribution, harmonic excitation, dynamic amplification, the Von Mises (VM) failure criterion, and Monte Carlo simulation to investigate how uncertain excitation frequencies and resonance influence the probability of failure.

The probabilistic model is fully defined by specifying the physical meaning, mean value, standard deviation, coefficient of variation, and probability distribution of each random variable. In the absence of experimental covariance data, all variables are assumed statistically independent. Mechanical and geometric parameters follow Gaussian distributions, whereas the excitation frequency is uniformly distributed within each analyzed frequency band, consistent with the original MATLAB implementation.

2 Physical Problem and Structural Idealization

The Cessna 172 wing spar is idealized as the primary longitudinal element of the wing. The model neglects the detailed interaction with ribs, skin panels, secondary spars, joints, and local stress concentrations. The adopted structural idealization is a cantilever beam fixed at the fuselage and free at the wing tip.

The adopted spar length is $L = 4.95\ m$, corresponding to half of the effective wing span. The I-section is defined by height $h = 0.15\ m$, flange widths $b_t = b_b = 0.10\ m$, flange thicknesses $t_t = t_b = 0.01\ m$, and web thickness $t_w = 0.005\ m$. The material is aluminum 2024-T3, with nominal elastic modulus $E = 73.1\ GPa$, density $\rho = 2760\ kg/m^3$, and yield stress $\sigma_y = 345\ MPa$.

For the symmetric I-section, the cross-sectional area is

$$A = b_t t_t + b_b t_b + t_w(h - t_t - t_b). \tag{1}$$

The second moment of area about the bending axis is

$$I = \frac{b_t t_t^3}{12} + b_t t_t \left(\frac{h}{2} - \frac{t_t}{2}\right)^2 + \frac{b_b t_b^3}{12} + b_b t_b \left(\frac{h}{2} - \frac{t_b}{2}\right)^2 + \frac{t_w(h - t_t - t_b)^3}{12}. \tag{2}$$

The first moment of area adopted for shear stress evaluation is

$$Q = b_t t_t \left(\frac{h}{2} - \frac{t_t}{2}\right) + \frac{t_w(h - t_t - t_b)}{2} \left(\frac{h - t_t - t_b}{4}\right). \tag{3}$$

The simplified torsional constant is written as

$$J = 2\frac{b_t t_t^3}{3} + 2\frac{b_b t_b^3}{3} + \frac{t_w(h - t_t - t_b)^3}{3}. \tag{4}$$

These expressions are used inside the Monte Carlo loop. Therefore, the stiffness and stress response change from one sample to another as the random geometry changes.

3 Aerodynamic Loading and Internal Forces

For level flight, the total lift is assumed to equal the aircraft weight, $W = mg$, where $m = 1160\,\mathrm{kg}$. The lift distribution along the half span is assumed to be elliptical.

$$q(x) = q_{\max}\sqrt{1 - \left(\frac{x}{L}\right)^2}, \quad 0 \le x \le L, \tag{5}$$

where $x = 0$ corresponds to the wing root. Only a fraction of the total wing load is assigned to the main spar, because skin, ribs, and secondary members also participate in the load path.

The shear force, bending moment, and torsional moment are obtained by:

$$V(x) = \int_x^L q(s)\,ds, \qquad M(x) = \int_x^L q(s)(s-x)\,ds, \qquad T(x) = e\,V(x). \tag{6}$$

where e is the eccentricity between the resultant lift and the reference axis of the spar. The critical section is the root, where both shear force and bending moment reach their maximum values. Figure 1 presents the loading and resulting internal forces, based on the same mathematical model used in the original work.

4 Random Variables and Probabilistic Model

4.1 General assumption

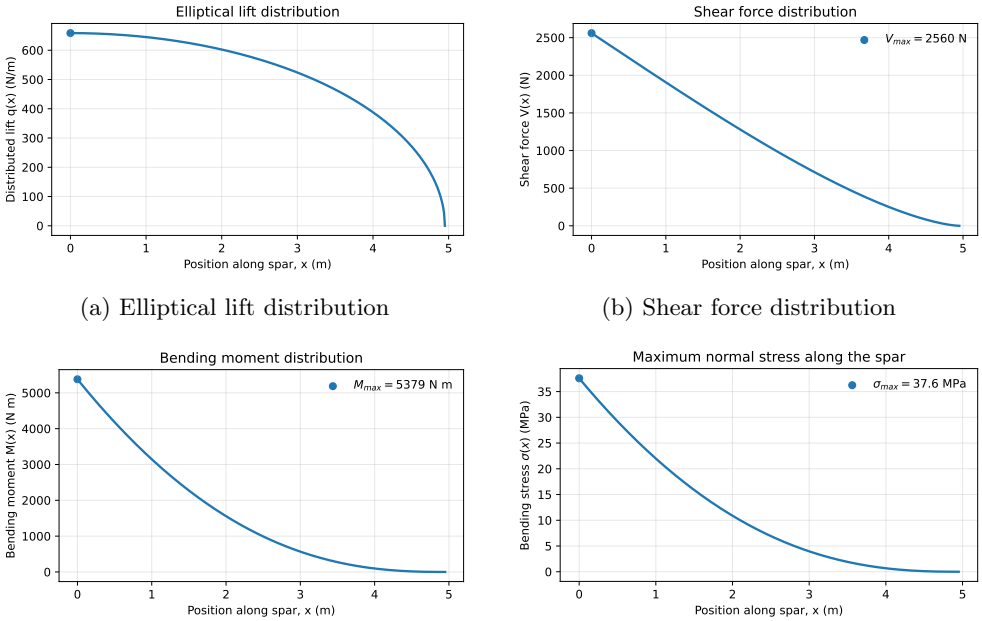
The uncertainty model is defined by the random vector $\boldsymbol{X} = [h, b_t, b_b, t_t, t_b, t_w, E, \sigma_y, \rho, q_0, e, f_{exc}]^T$, which contains the geometric dimensions, material properties, aerodynamic loading, and excitation frequency. The uncertainty model contains two classes of statistically independent variables. The first class includes the geometric, material, and loading variables, which are modeled as Gaussian variables:

$$X_i \sim \mathcal{N}(\mu_i, \sigma_i^2), \quad i = 1, 2, \ldots, n_g, \tag{7}$$

where μ_i is the mean value and σ_i is the standard deviation of the i-th Gaussian variable. The second class is the excitation frequency, which is not Gaussian in the MATLAB implementation. For each simulation test j, it is sampled from a uniform distribution within the prescribed band:

$$f_{exc}^{(j)} \sim U\left(f_{min}^{(j)}, f_{max}^{(j)}\right). \tag{8}$$

Thus, any frequency inside the interval has the same probability of occurrence. This is an important modeling point: a test band such as 40–60 Hz does not represent a deterministic excitation at 50 Hz; it represents a random excitation frequency generated uniformly between 40 Hz and 60 Hz.



(a) Elliptical lift distribution

(b) Shear force distribution

(c) Bending moment distribution

(d) Maximum normal stress distribution

Fig. 1: Lift, shear, bending moment, and normal stress distribution along the spar

The joint probability density function is the product of the marginal densities because all variables are assumed independent [3]:

$$f_{\boldsymbol{X}}(\boldsymbol{x}) = \left[\prod_{i=1}^{n_g} \frac{1}{\sigma_i\sqrt{2\pi}} \exp\left[-\frac{1}{2}\left(\frac{x_i-\mu_i}{\sigma_i}\right)^2\right]\right] \frac{1}{f_{max}^{(j)} - f_{min}^{(j)}}, \tag{9}$$

for $f_{min}^{(j)} \leq f_{exc} \leq f_{max}^{(j)}$; otherwise, the uniform frequency density is zero. The covariance matrix of the Gaussian subset is diagonal:

$$\boldsymbol{C}_{\boldsymbol{X_g}} = \operatorname{diag}\left(\sigma_1^2, \sigma_2^2, \ldots, \sigma_{n_g}^2\right), \tag{10}$$

with zero covariance between any pair of distinct Gaussian variables:

$$\operatorname{Cov}(X_i, X_k) = 0, \quad i \neq k. \tag{11}$$

The excitation frequency is also independent of the Gaussian variables.

This independence assumption is adopted because no experimental or manufacturing data are available to define correlation coefficients. Accordingly, the paper refers to "multiple random variables" rather than "correlated random variables". If correlation data become available, Equation 10 can be replaced by a full covariance matrix,

with random samples generated using an appropriate transformation, such as Cholesky decomposition.

4.2 Numerical values of the random variables

Table 1 presents the adopted stochastic model. The coefficient of variation is given by

$$\mathrm{COV}_i = \frac{\sigma_i}{\mu_i} \times 100\%. \tag{12}$$

The selected values define a preliminary reliability model. Geometric variables use small coefficients of variation consistent with manufacturing tolerances, while material properties and aerodynamic load adopt moderate and larger variations, respectively, to represent their uncertainties.

Table 1: Random variables adopted in the Monte Carlo simulation. All variables are assumed to be independent. Geometric, material, and load variables follow normal distributions, whereas the excitation frequency follows a uniform distribution within each prescribed frequency band

Symbol	Description	Unit	Mean μ	Std. dev. σ
h	Total spar height	m	0.1500	0.0030
b_t	Upper flange width	m	0.1000	0.0020
b_b	Lower flange width	m	0.1000	0.0020
t_t	Upper flange thickness	m	0.0100	0.0003
t_b	Lower flange thickness	m	0.0100	0.0003
t_w	Web thickness	m	0.0050	0.00015
E	Young's modulus	GPa	73.10	3.655
σ_y	Yield stress	MPa	345.0	17.25
ρ	Mass density	kg/m^3	2760	82.8
q_0	Reference distributed load	N/m	517.25	51.73
e	Load eccentricity	m	0.1000	0.0050
f_{exc}	Excitation frequency	Hz	Band-dependent	Band-dependent

The reference load q_0 represents the nominal distributed load associated with the spar lift contribution and scales the elliptical distribution in each Monte Carlo realization. Negative samples are physically inadmissible, but their probability is negligible with the adopted coefficients of variation. In practice, such samples can be rejected or modeled using truncated normal or lognormal distributions.

4.3 Excitation frequency model

The excitation frequency is a band-dependent uniform random variable. This definition follows the MATLAB implementation used in the original work, in which the excitation samples are generated by a command equivalent to

$$f_{exc} = f_{min} + (f_{max} - f_{min})\, U, \quad U \sim U(0,1). \tag{13}$$

Therefore,

$$f_{exc} \sim U(f_{min}, f_{max}). \tag{14}$$

The probability density function is

$$f_{f_{exc}}(f) = \begin{cases} \dfrac{1}{f_{max} - f_{min}}, & f_{min} \leq f \leq f_{max}, \\ 0, & \text{otherwise.} \end{cases} \tag{15}$$

For a uniform variable in the interval $[a, b]$, the mean and standard deviation are

$$\mu_f = \frac{a+b}{2}, \quad \sigma_f = \frac{b-a}{\sqrt{12}}. \tag{16}$$

These values are descriptive only; the actual sampling follows a uniform distribution.

The statistical model for each excitation test is presented in Table 2. For the broad-band case, the model is $f_{exc} \sim U(0, 200)$ Hz, which gives $\mu_f = 100\ Hz$ and $\sigma_f = 57.74\ Hz$.

Table 2: Uniform model for the excitation frequency in each simulation test

Test	Frequency band (Hz)	μ_f (Hz)	σ_f (Hz)	Distribution
1	0–20	10	5.77	Uniform, independent
2	20–40	30	5.77	Uniform, independent
3	40–60	50	5.77	Uniform, independent
4	60–80	70	5.77	Uniform, independent
5	80–100	90	5.77	Uniform, independent
6	100–120	110	5.77	Uniform, independent
7	120–140	130	5.77	Uniform, independent
8	140–160	150	5.77	Uniform, independent
9	160–180	170	5.77	Uniform, independent
10	180–200	190	5.77	Uniform, independent
11	0–200	100	57.74	Uniform, independent

4.4 Sampling algorithm

For each Monte Carlo sample k, independent standard normal variables are generated for the Gaussian subset:

$$Z_i^{(k)} \sim \mathcal{N}(0, 1), \quad i = 1, 2, \ldots, n_g. \tag{17}$$

The corresponding physical variables are obtained by

$$X_i^{(k)} = \mu_i + \sigma_i Z_i^{(k)}. \tag{18}$$

The excitation frequency is sampled independently through

$$f_{exc}^{(k)} = f_{min}^{(j)} + \left(f_{max}^{(j)} - f_{min}^{(j)} \right) U^{(k)}, \quad U^{(k)} \sim U(0, 1). \tag{19}$$

The sequence of calculations for each sample is:

1. generate independent normal realizations of geometric, material, and load variables;
2. compute A, I, Q, and J from the sampled geometry;
3. compute $q(x)$, $V(x)$, $M(x)$, and $T(x)$ from the sampled load and eccentricity;
4. compute the natural frequencies from the sampled E, ρ, A, and I;
5. sample f_{exc} within the selected frequency band and compute R;
6. compute the amplified stress components and the equivalent Von Mises stress;
7. evaluate the performance function $G(\boldsymbol{X})$;
8. count failure if $G(\boldsymbol{X}) < 0$.

5 Stress Model and Dynamic Amplification

At each Monte Carlo realization, the bending normal stress, transverse shear stress, and torsional shear stress are evaluated, respectivelly, as

$$\sigma = \frac{Mc}{I}, \qquad \tau = \frac{VQ}{It_w}, \qquad \tau_t = \frac{Tr}{J}. \tag{20}$$

where $c = \frac{h}{2}$ and r is a representative radial distance for the torsional contribution.

The natural frequencies are approximated by the Euler-Bernoulli cantilever beam expression [4]

$$\omega_n = \lambda_n^2 \sqrt{\frac{EI}{m' L^4}}, \quad f_n = \frac{\omega_n}{2\pi}, \tag{21}$$

where $m' = \rho A$ is the mass per unit length. The first three modal constants are $\lambda_1 = 1.875$, $\lambda_2 = 4.694$, and $\lambda_3 = 7.855$. The mean natural frequencies obtained in the study were approximately 7.47 Hz, 46.81 Hz, and 131.09 Hz.

The dynamic amplification factor for a given mode is written as [5]

$$R_n = \frac{1}{\sqrt{(1 - r_n^2)^2 + (2\zeta r_n)^2}}, \quad r_n = \frac{f_{exc}}{f_n}, \tag{22}$$

with damping ratio $\zeta = 0.06$. To avoid nonphysical simultaneous resonance of all vibration modes, the modal amplification factors were averaged:

$$R = \frac{1}{n_m} \sum_{n=1}^{n_m} R_n. \tag{23}$$

The amplified stress components are therefore

$$\sigma_d = R\sigma, \quad \tau_d = R\tau, \quad \tau_{t,d} = R\tau_t. \tag{24}$$

The equivalent Von Mises stress is

$$\sigma_{VM} = \sqrt{\sigma_d^2 + 3(\tau_d + \tau_{t,d})^2}. \tag{25}$$

6 Reliability and Monte Carlo Simulation

The limit-state function is defined as

$$G(\boldsymbol{X}) = \sigma_y - \sigma_{VM}(\boldsymbol{X}), \tag{26}$$

where $\boldsymbol{X}$ is the vector of random variables [2]. Failure occurs when $G(\boldsymbol{X}) < 0$.

For N Monte Carlo samples, the failure probability is estimated by $P_f = \frac{N_f}{N}$, where N_f is the number of failed samples. The reliability index is computed as $\beta = \frac{\mu_G}{\sigma_G}$, where μ_G and σ_G are the sample mean and standard deviation of $G(\boldsymbol{X})$ [2].

The numerical implementation used $N = 100000$ simulations. This sample size is consistent with standard Monte Carlo reliability applications reported in the literature [6]. The first ten tests considered 20 Hz excitation bands from 0 to 200 Hz, with f_{exc} uniformly sampled within each interval. An additional test evaluated the full 0–200 Hz range to represent a broader operational excitation spectrum.

7 Results

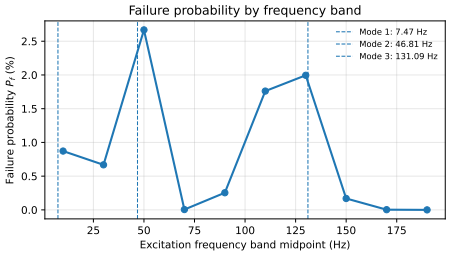
Table 3 summarizes the reliability results. The values of P_f and β are interpreted together: low P_f and high β indicate safe behavior, whereas bands close to natural frequencies produce stress amplification and lower reliability.

Table 3: Summary of Monte Carlo reliability results

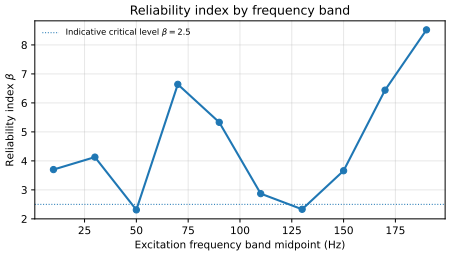
Test (Hz)	β	P_f (%)	Mean σ_{VM} (MPa)
1 (0–20)	3.70	0.8720	64.27
2 (20–40)	4.13	0.6680	60.22
3 (40–60)	2.31	2.6680	97.39
4 (60–80)	6.64	0.0050	43.88
5 (80–100)	5.33	0.2540	46.86
6 (100–120)	2.87	1.7610	77.39
7 (120–140)	2.33	1.9950	100.65
8 (140–160)	3.66	0.1690	64.76
9 (160–180)	6.44	0.0030	31.70
10 (180–200)	8.52	0.0000	18.64
11 (0–200)	3.38	0.8520	60.67

Figure 2 shows that the largest failure probabilities occur in frequency ranges close to the second and third natural frequencies. The stress trend follows the same behavior: higher mean Von Mises stresses are observed in the bands containing the main resonance regions.

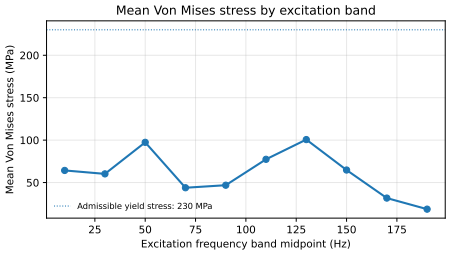
The stress-frequency plot in Figure 3a shows higher stresses near the modal frequencies, particularly the second and third modes, indicating that failure probability is concentrated in dynamically critical regions. Consistently, Figure 3b shows that most samples remain in the positive domain, while the small fraction below zero represents the failure probability.



(a) Failure probability

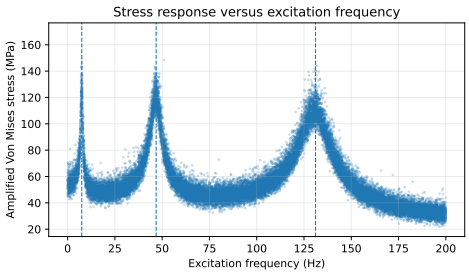


(b) Reliability index

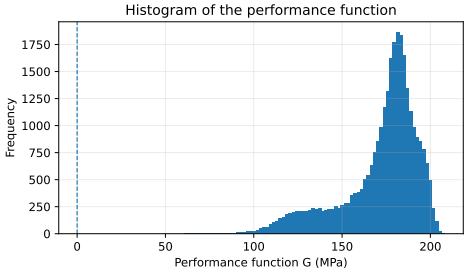


(c) Mean Von Mises stress

Fig. 2: Reliability indicators as functions of excitation band



(a) Amplified VM stress as a function of f_{exc}



(b) Histogram of the performance function

Fig. 3: Results for the Von Mises stress and histogram of the performance function

8 Discussion and Conclusions

A Monte Carlo reliability analysis of the Cessna 172 main wing spar was performed considering uncertainties in geometry, material properties, loading, and dynamic excitation. The results show that reliability is strongly governed by the relationship between excitation and natural frequencies, with the second and third modes defining the most critical resonance bands. Off-resonance regions exhibit negligible P_f.

The broad-band simulation over 0–200 Hz yielded $P_f = 0.852\%$ and $\beta = 3.38$, indicating satisfactory reliability under the adopted assumptions. While narrow-band

analyses identify critical resonance regions, broad-band simulations provide an overall structural reliability measure.

The probabilistic model assumed independent random variables, with Gaussian distributions for geometry, material, and load parameters and a uniform distribution for excitation frequency. An averaged modal amplification factor was adopted to avoid unrealistic amplification from simultaneous modal resonance.

Despite neglecting aeroelastic coupling, fatigue, and structural interactions, the framework provides a practical approach for preliminary reliability assessment of aerospace structures under dynamic uncertainty.

Declarations

Funding

Not applicable.

Availability of data and material

Not applicable.

Competing interests

The authors declare that they have no competing interests.

Authors Contributions

M.A.S. and I.P. conducted the original research. M.A.S. and J.V. wrote the manuscript and prepared the figures and tables. J.V. and M.A.S. reviewed the manuscript.

References

[1] Megson, T.H.G.: Aircraft Structures for Engineering Students. Aerospace Engineering. Butterworth-Heinemann, Oxford (2021)

[2] Ditlevsen, O., Madsen, H.: Structural Reliability Methods. John Wiley & Sons Ltd, Chichester (1996)

[3] Haldar, A., Mahadevan, S.: Probability, Reliability, and Statistical Methods in Engineering Design. Wiley, New York (2000)

[4] Rao, S.S.: Vibration of Continuous Systems. Wiley, New Jersey (2019)

[5] Weaver, W., Timoshenko, S.P., Young, D.H.: Vibration Problems in Engineering. A Wiley-Interscience publication. Wiley, New York (1991)

[6] Rubinstein, R.Y., Kroese, D.P.: Simulation and the Monte Carlo Method. Wiley Series in Probability and Statistics. Wiley, New Jersey (2016)